Identification and quantitative analyses of microRNAs located in the distal axons of sympathetic neurons

ORLANGIE NATERA-NANJO,[1] ARMAZ ASCHRAFI,[1] ANTHONY E. GIOIO, and BARRY B. KAPLAN
Laboratory of Molecular Biology, National Institute of Mental Health, National Institutes of Health, Bethesda, Maryland 20892-1381, USA

ABSTRACT

microRNAs (miRNAs) constitute a novel class of small, noncoding RNAs that act as negative post-transcriptional regulators of gene expression. Although the nervous system is a prominent site of miRNA expression, little is known about the spatial expression profiles of miRNAs in neurons. Here, we employed compartmentalized Campenot cell culture chambers to obtain a pure axonal RNA fraction of superior cervical ganglia (SCG) neurons, and determined the miRNA expression levels in these subcellular structural domains by microarray analysis and by real-time reverse-transcription polymerase chain reaction. The data revealed stable expression of a number of mature miRNAs that were enriched in the axons and presynaptic nerve terminals. Among the 130 miRNAs identified in the axon, miR-15b, miR-16, miR-204, and miR-221 were found to be highly abundant in distal axons as compared with the cell bodies of primary sympathetic neurons. Moreover, a number of miRNAs encoded by a common primary transcript (pri-miRNA) were differentially expressed in the distal axons, suggesting that there is a differential subcellular transport of miRNAs derived from the same coding region of the genome. Taken together, the data provide an important resource for future studies on the regulation of axonal protein synthesis and the role played by miRNAs in the maintenance of axonal structure and function as well as neuronal growth and development.

Keywords: superior cervical ganglion; primary neurons; microRNA; microarray profiling; real-time PCR; target mRNAs

INTRODUCTION

Subcellular mRNA localization comprises a fundamental mechanism for regulated gene expression in developing and adult brain. The resulting temporal and spatial patterns of local protein synthesis is required for a number of important neuronal processes, such as differentiation and maturation, axon guidance, synapse formation, and cognitive brain functions (Costa-Mattioli et al. 2009). Previous studies identified that local translation is under tight control via a number of different mechanisms, such as control of mRNA stability (Smart et al. 2007), translation initiation (Klann et al. 2004), and elongation (Huang et al. 2005) and by the recently discovered noncoding miRNAs (for review, see Schratt 2009a). At present, there is little knowledge of the intricate nature and role played by miRNAs in the axons and synaptic terminals of neurons. The regulation of

gene expression by miRNAs represents a distinct mechanism of translation regulation. miRNAs are single-stranded RNA moieties of about 21–23 nucleotides (nt) in length. They are highly conserved and involved in a subset of biological processes in which they have been shown to be implicated in developmental timing, cell proliferation, apoptosis, metabolism, cell differentiation, and morphogenesis (Ambros and Lee 2004; Niwa and Slack 2007). Several recent reviews provide detailed descriptions of miRNA biogenesis and mode of action (Kim 2005; Filipowicz et al. 2008). Remarkably, it has been shown that these small molecules coordinately regulate multiple genes coding for proteins with related cellular functions (van Rooij and Olson 2007), and their presence in the dendrites of neurons has been previously reported (Kye et al. 2007; Lugli et al. 2008; Siegel et al. 2009).

The functions of individual miRNAs in neurons are just beginning to emerge, and multiple lines of evidence point to the widespread involvement of miRNAs in various neurological diseases (for review, see Bassell and Warren 2008; Hunsberger et al. 2009). In addition, recent studies have elucidated several roles for neural miRNAs at various stages of synaptic development, including dendritogenesis, synapse formation, and synapse maturation. Furthermore, some of

---

these studies have shown that miRNAs regulate mRNA translation locally in the synaptodendritic compartment (for review, see Schratt 2009b). In recent studies, we delineated a novel molecular mechanism by which the brain-specific miR-338 participated in the regulation of axonal growth and function by locally modulating the levels of a nuclear-encoded mitochondrial protein. This finding points to a novel mechanism for a soma-independent regulation of protein synthesis in distal axons through neuronal miRNAs (Aschrafi et al. 2008).

In the present study, we employed a compartmentalized cell culture system to obtain a pure axonal RNA fraction of superior cervical ganglia (SCG) neurons, and present the results of a microarray analysis that led to the identification of a large heterogeneous population of axonal miRNAs. By combining microarray expression profiling with miRNA-specific real-time reverse-transcription polymerase chain reaction (RT-PCR), we provide, for the first time, a comprehensive list of miRNAs residing within the axonal domain. These data provide a base for future studies of individual miRNAs, their target genes, and the role played by the miRNAs in the regulation of local protein synthesis.

RESULTS AND DISCUSSION

Although we routinely monitor the side compartments of the Campenot cell culture chambers for the presence of neuronal cell soma and non-neuronal cells using light microscopy, trace cellular contamination of the axonal RNA preparation might still be detectable at the level of resolution afforded by microarray analysis or real-time PCR methodology. To address this issue, the purity of the RNA samples prepared from the distal axons was assessed by real-time PCR using gene-specific primer sets for mRNAs present in neuronal cell soma and glia. As shown in Figure 1A, amplicons for *munc18*, *rim*, and *synapsin 3*, mRNAs encoding proteins involved in synaptic vesicle function,

were readily visualized in RNA prepared from the neurons present in the central compartment, but were not observed in RNA obtained from distal axons. Identical results were obtained using gene-specific primers for glial fibrillary acidic protein (Fig. 1A, GFAP). These data support the contention that the RNA prepared from the side compartments is free of neuronal and glial contamination.

Results of Western blot analysis performed on protein lysates obtained from the side and central compartments of the Campenot chambers indicate that the distal axonal fraction is enriched for axonal proteins (Fig. 1B). For example, the abundance of Tau, an axonal marker protein, relative to β-actin, was greater in the distal axons as compared with the neuronal soma (relative ratio axon to soma 4:1). In contrast, distal axons were devoid of MAP2, whereas this dendritic biomarker was readily detected in protein samples obtained from the central compartment (Fig. 1B).

Previously, we identified an axonally localized miRNA that regulates the expression of cytochrome *c* oxidase IV (COXIV), a key protein within the electron transfer chain in mitochondria, which participates in the control of ATP levels in the axons of sympathetic neurons (Li et al. 2006; Aschrafi et al. 2008). We reasoned that miRNAs that are important for axonal function and development might be located in distal axons, where they could locally regulate the translation of relevant target mRNAs. To investigate the global expression of miRNAs in the axons of primary SCG neurons, we isolated total RNA from the distal axons of SCG neurons, and delineated the component miRNAs using a miRNA microarray kit with optimized probe sequences targeting all of the known mature rat miRNAs in the miRBase Sequence Database, Release 9.0. In addition, we analyzed total RNA from the central compartments of these cultures, which contained the parental cell bodies and proximal axons of these neurons. Microarray expression profiling revealed that axons of rat sympathetic neurons contain a large, heterogeneous population of miRNAs (Supplemental Table S1): Several of these miRNAs are highly expressed in these neurons. A listing of miRNAs that are most abundant and/or enriched in the axon is provided in Table 1. In addition, the microarray data demonstrated that miRNAs belonging to the same family could be readily differentiated by this experimental approach. For example, miR-125a and miR-125b differ only by three nucleotides, but yielded highly reliable and markedly different signal intensities of 41.2 ($\pm$5.2 SEM) and 322.5 ($\pm$43.8 SEM) relative fluorescence units (RFU), respectively.

To further assess the distribution of the miRNAs in the axons as compared with cell bodies, we calculated the ratios
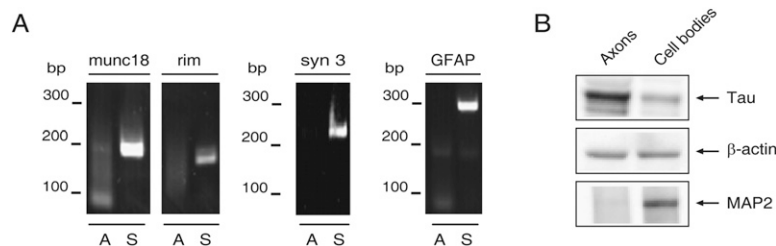
FIGURE 1. RNA prepared from the distal axons of SCG neurons is free of neuronal and glial contamination. (*A*) RT-PCR analysis was conducted on RNA obtained from the lateral and central compartments of the Campenot cell culture chambers using gene-specific primer sets for synaptic vesicle proteins, munc18, rim, synapsin 3 (syn 3), and glial fibrillary acidic protein (GFAP). PCR products were fractionated on 2.5% agarose gels and amplicons visualized by ethidium bromide staining. (A) Axon; (S) soma; (bp) base pairs. (*B*) Protein lysates obtained from the lateral and central compartments of the Campenot chambers were analyzed by Western blot using antibodies against Tau and MAP2. Levels of β-actin immunoreactivity served as an internal control.

TABLE 1. List of select relatively abundant or enriched axonal miRNAs as assessed by microarray analysis[a]

miRNA name	Axon intensity	Soma intensity	Ratio of intensities (axon/soma)
rno-miR-125b	322.50 ± 43.75	247.67 ± 42.67	1.35 ± 0.15
rno-miR-382	132.33 ± 9.83	165.17 ± 14.49	0.85 ± 0.12
rno-miR-23a	126.17 ± 11.70	97.17 ± 11.49	1.33 ± 0.12
rno-miR-23b	125.67 ± 3.91	108.50 ± 10.98	1.16 ± 0.12
rno-miR-24	83.50 ± 9.30	106.83 ± 18.77	0.84 ± 0.11
rno-miR-329	43.00 ± 4.57	95.50 ± 15.66	0.48 ± 0.04
rno-miR-26a	41.67 ± 2.63	33.83 ± 2.48	1.24 ± 0.06
rno-miR-221	41.17 ± 4.50	7.17 ± 0.83	5.83 ± 0.49
rno-miR-16	34.33 ± 1.86	9.83 ± 3.13	3.69 ± 0.35
rno-miR-185	33.67 ± 0.67	55.83 ± 5.18	0.62 ± 0.05
rno-miR-103	32.50 ± 2.14	18.33 ± 1.33	1.81 ± 0.15
rno-miR-127	31.33 ± 3.17	23.00 ± 3.81	1.44 ± 0.15
rno-miR-320	31.17 ± 2.02	14.33 ± 1.65	2.29 ± 0.24
rno-miR-541	27.67 ± 1.99	20.33 ± 2.74	1.49 ± 0.21

Enriched miRNAs manifest axon/soma intensity ratios >1.0.
[a]Microarray data are shown as average of six replicates (±SEM).

of the axonal signal intensities compared with the signal intensities in the cell body for each miRNA. The distribution pattern for 60 miRNAs is shown in Figure 2A. The average ratio (axon/soma) obtained for the miRNAs by microarray profiling was 1.26 (±0.08 SEM), suggesting that most miRNAs have similar relative abundances between the cell bodies and distal axons. However, a number of miRNAs were observed that were significantly enriched in the axons compared with the cell bodies, while others were enriched or present only in the cell bodies. For example, miR-204, miR-221, miR-15b, and miR-16 are characterized by the former pattern, while miR-297, miR-206, and miR-124a are examples of the latter pattern. This finding confirmed previous studies reporting that miR-124a, a miRNA important for neuronal differentiation, is cell-body restricted, as assessed by microarray analysis, in situ hybridization (ISH), and RT-PCR (Kye et al. 2007; Siegel et al. 2009).

To validate the microarray analysis, we assessed the expression of 57 miRNAs by real-time quantitative RT-PCR (qRT-PCR) using miRNA-specific primers. As selection criteria, we chose miRNAs found to be highly expressed by microarray, with axonal signal intensities that were three standard deviations above the background intensity, as well as some that were expressed at a lower level, with signal intensities that were one to two standard deviations above background. In addition, 17 miRNAs with microarray intensities less than one standard deviation above background level were assayed by qPCR to establish a cutoff C_T value. Previously, it was shown that mature miRNAs present in low copy number have C_T values higher than 35 (Schmittgen et al. 2008). Consistent with this finding, the C_T values obtained for 16 of these miRNAs

were higher than 36, and the corresponding standard deviations were high (≥1). Additionally, melting curve analyses of the amplicons revealed a lack of fidelity of the signal. A rank ordering of the 15 most abundant miRNAs, as judged by qRT-PCR analysis (C_T values), is provided in Table 2.

Following the establishment of the cutoff C_T value, we calculated the relative expression (RQ) of the miRNAs in the axons compared with the soma using the comparative C_T method (Schmittgen and Livak 2008). This method has been successfully employed in the quantitative analyses of miRNA expression by real-time PCR (Saba et al. 2008; Schmittgen et al. 2008; Aldrich et al. 2009; Hébert et al. 2009). Briefly, ΔC_T values for each miRNA were obtained after normalizing to U6 snRNA, a common normalizer for miRNA expression, and miR-103, which has been previously shown to be a very stable reference miRNA (Peltier and Latham 2008). The RQ for each miRNA in the axon compared with the soma was calculated using the equation $2^{-\Delta\Delta C_T}$, where $\Delta\Delta C_T = \Delta C_{T,axon} - \Delta C_{T,soma}$ (for example, see Table 2). As shown in Figure 2B, the analyzed miRNAs were distributed between cell bodies and axons in a Gaussian fashion similar to the distribution calculated for miRNAs identified using microarray profiling. These studies further revealed a high correlation between the microarray profiling data and the results of real-time RT-PCR for more than 80% of the miRNAs (r = 0.73, P < 0.0001). Consistent with the microarray results, the average relative abundance of axonal/somal miRNA obtained by real-time RT-PCR analysis was 1.2(±0.1 SEM)-fold. Moreover, we were able to confirm the axonal enrichment of miR-204, miR-221, miR-15b, and miR-16 and the cell body enrichment of miR-297, miR-206, and miR-124a. However, in a few cases, inconsistencies between the microarray data and the real-time RT-PCR results were identified. For example, miR-329 showed a 2.6-fold axonal enrichment by real-time RT-PCR, but the ratio of intensities (axon/soma) obtained by microarray was 0.48(±0.04 SEM). Reasons for these discrepancies in the data are unclear, but could derive from differences in hybridization efficiencies or variations in RNA sampling.

To confirm the axonal localization of relatively abundant miRNAs identified by both microarray and qRT-PCR analyses, we performed ISH in primary SCG neurons, using locked nucleic acid (LNA) probes for miR-16, miR-221, and a scrambled miR probe as a negative control. Consistent with the microarray and real-time qPCR results, miR-16 and miR-221 were readily visualized in distal axons as punctate fluorescent ISH signals (Fig. 3A,B). In contrast,
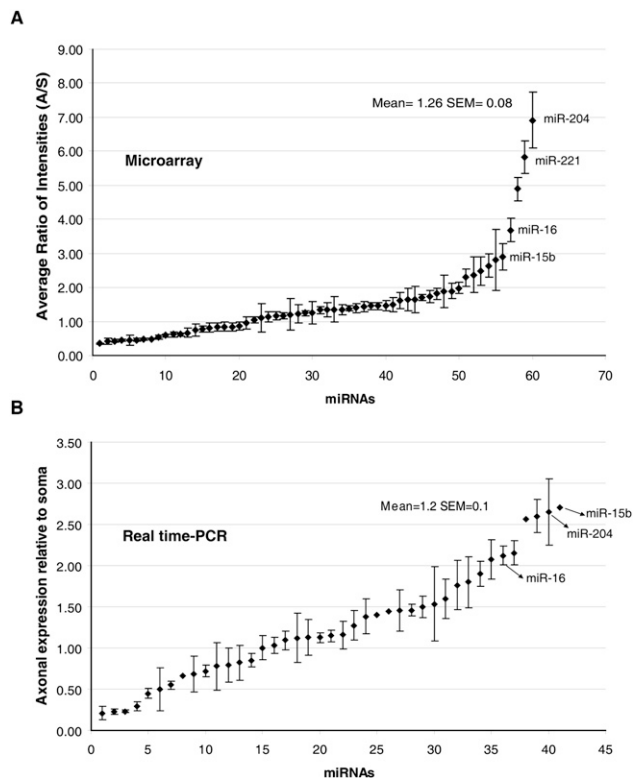
FIGURE 2. A comparison of the abundance ratios (axon/soma) of miRNAs expressed in axons as judged by microarray analysis and qRT-PCR. (*A*) miRNA expression in the axons assessed by microarray. The average ratios of axonal miRNA intensities relative to miRNA intensity in the soma were calculated for 60 miRNAs. Error bars represent the standard error of mean (SEM) of six replicates. (*B*) miRNA expression in the axons assessed by real-time RT-PCR. Distribution plot shows the relative expression of axonal miRNAs compared with the soma as measured using miRNA-specific primers. Relative expression was calculated using the $2^{-\Delta\Delta C_T}$ value after normalizing the C_T values in the axons and soma to the corresponding levels of U6 snRNA. The distribution can be approximated as normal by means of the Shapiro-Wilk normality test ($P = 0.286$).

no punctate fluorescent signals were observed with the scrambled miR probe (Fig. 3C).

An essential requirement for the functional role of miRNAs at post- or presynaptic endings is the targeted delivery of these noncoding RNAs along the neuronal processes. However, the mechanism of miRNA transport is entirely unknown. Several models were proposed for the shuttling of miRNAs to the synapse (Kosik 2006). The models proposed included codelivery of miRNAs with their cognate mRNA targets into neuronal endings by RNA granules, mRNA-independent delivery of mature miRNAs, as well as synaptic delivery of the precursor miRNA molecules, followed by a subsequent local processing by Dicer to the mature functional miRNA form. The latter model is supported by our previous findings of the presence of miRNA processing machinery in distal axons of sympathetic neurons (Aschrafi et al. 2008).

Many of the known miRNAs appear in clusters on a single polycistronic transcript (Lagos-Quintana et al. 2003). Although post-transcriptional regulation of miRNA expression has been demonstrated (Obernosterer et al. 2006), little is known about the regulation and processing of different miRNAs derived from the same transcript. In this study, we explored the relative distribution of miRNAs derived from 13 polycistronic transcripts. Our results indicate that the relative abundance of some of the miRNAs derived from five polycistronic gene transcripts differed significantly in the axon and cell soma (Table 3). This finding suggests that only a subset of polycistronically expressed miRNAs are post-transcriptionally regulated and differentially transported into the distal axons. Alternatively, the half-lives of these miRNAs might differ markedly in the two cell compartments. Whether the selective expression of polycistronically expressed miRNAs is an axon-specific phenomenon or is manifest in the dendrites is unclear, and represents an interesting question for future research.

miRNAs fine-tune the expression of their target genes in disperse locations within the cell. A particularly powerful aspect of miRNA function is the ability of individual miRNAs to coordinately regulate a multitude of genes coding for proteins with related cellular functions. Based upon this observation, we explored the possibility that miRNAs that were highly abundant or enriched in the axon had putative target genes with similar axonal functions. Using the miRNA target prediction tool TargetScan (Lewis et al. 2005), we identified putative targets for miR-204, miR-221, miR-146, miR-16 and miR-15b, miR-320, miR-103, miR-541, miR-125b, miR-23a and miR-23b, miR-26a,

TABLE 2. Abundance rank ordering of axonal miRNAs as assessed by qRT-PCR analysis

miRNA name	Average C_T[a]		Relative expression $(2^{-\Delta\Delta C_T})$[b]
	Axon	Soma	
rno-miR-23b	25.04 ± 0.08	20.05 ± 0.18	1.46 ± 0.07
rno-miR-125b	27.13 ± 0.20	21.12 ± 0.14	0.72 ± 0.07
rno-miR-23a	27.79 ± 0.12	22.69 ± 0.07	2.12 ± 0.11
rno-miR-329	28.37 ± 0.16	24.20 ± 0.04	2.60 ± 0.20
rno-miR-24	28.60 ± 0.55	21.75 ± 0.04	0.79 ± 0.21
rno-miR-127	29.80 ± 0.14	23.73 ± 0.21	1.03 ± 0.10
rno-miR-320	29.82 ± 0.39	24.12 ± 0.25	1.76 ± 0.30
rno-miR-185	30.65 ± 0.07	23.90 ± 0.09	0.85 ± 0.08
rno-miR-26a	30.79 ± 0.44	25.42 ± 0.18	1.13 ± 0.22
rno-miR-541	30.92 ± 0.29	24.60 ± 0.06	1.15 ± 0.07
rno-miR-103	31.09 ± 0.33	24.58 ± 0.03	1.00 ± 0.15
rno-let-7c	31.25 ± 0.25	24.86 ± 0.05	1.09 ± 0.11
rno-miR-221	31.41 ± 0.33	25.38 ± 0.18	1.41 ± 0.02
rno-miR-382	31.46 ± 0.18	26.21 ± 0.07	1.90 ± 0.15
rno-miR-16	31.53 ± 0.31	26.12 ± 0.12	2.16 ± 0.15

[a]C_T values are the average of three replicates (±SD).
[b]Relative expression as calculated by the comparative threshold method (Schmittgen and Livak 2008), and as delineated in the Materials and Methods section.
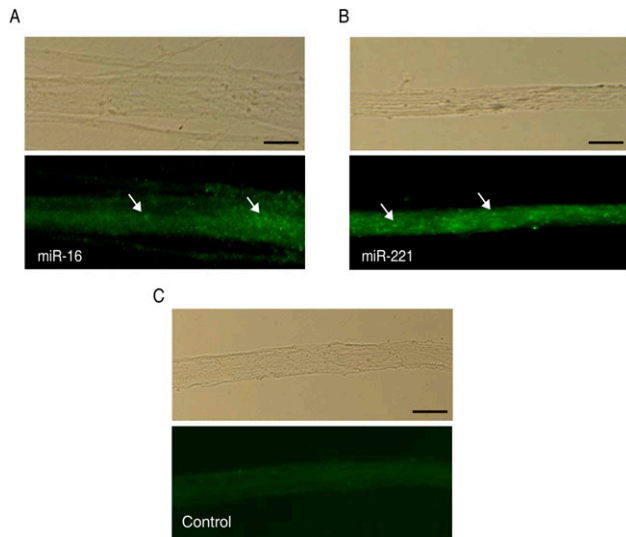
FIGURE 3. Visualization of miRNAs in distal axons by in situ hybridization (ISH). ISH was performed in primary SCG neurons at 7 d in vitro (DIV) using fluorescein isothiocyanate (FITC)-conjugated LNA probes for miR-16 (A), miR-221 (B), and a scrambled miR probe as a negative control (C). Arrows indicate the location of punctate ISH signals in distal axons for miR-16 and miR-221. Scale bars, 10 μm. Phase contrast images of the axon fibers are provided in the corresponding *top* panels.

miR-382, miR-24, and miR-185 (Table 4). Many of these target genes coded for receptors and ion channels, molecular motors, transcription and translation factors, ribosomal proteins, as well as proteins involved in vesicle recycling. All of these putative target mRNAs have been identified in the axons of invertebrates (Martin 2004; Crispino et al. 2009) and vertebrates (Willis et al. 2007; Taylor et al. 2009; Vogelaar et al. 2009). It is important to note that receptors and transmembrane proteins can be synthesized locally in axons (Spencer et al. 2000; Bi et al. 2006; Tsai et al. 2006) and that functional receptors appear to be incorporated into the axolemma via an ER- and Golgi-dependent mechanism (Merianda et al. 2009).

Although attention has been focused on miRNAs that are relatively abundant or enriched in the axon in this report (Table 1), it is likely that low abundance miRNAs might also play an important role in the regulation of local translation and axonal function. For example, the axonal localization of brain-specific miR-338 has been established by in-situ hybridization histochemistry using LNA hybridization probes, and has been shown to regulate axonal ATP synthesis and respiration in SCG neurons through modulation of COXIV mRNA levels (Aschrafi et al. 2008).

Protein translation in neurons occurs in the cell bodies or locally in the distal neuronal processes. Local protein synthesis is implicated in many aspects of neuronal development and function, such as axon guidance, dendritic elaboration, synaptic plasticity, and long-term memory formation. Although the existence of local translation in

dendrites has been widely accepted, the question of whether or not translation occurs in axons has remained more controversial. Recent findings establish that proteins requisite for structural/functional maintenance of axons are synthesized locally in the axon and nerve terminal, and call attention to the intimacy of the relationship that has evolved between the distant cellular domains of the neuron and its local protein synthetic system (for review, see Kaplan et al. 2009).

In conclusion, our studies delineated the miRNAs present in the axons of sympathetic neurons, and provide an important resource for future studies on the role played by miRNAs in the regulation of intra-axonal protein synthesis.

MATERIALS AND METHODS

Neuronal cell culture

SCG were obtained from 3-d-old Harlan Sprague Dawley rats, and dissociated neurons plated in the central compartment of

TABLE 3. Overview of the ratios of intensities (axon/soma) for polycistronically expressed miRNAs[a]

miRNA	Ratio of intensities (axon/soma)
miR-433-127 cluster	
rno-miR-433	1.71 ± 0.09
rno-miR-127	1.44 ± 0.15
rno-miR-136	0.80 ± 0.34[*]
miR-379-410 cluster	
rno-miR-379	0.45 ± 0.15
rno-miR-329	0.48 ± 0.04
rno-miR-487b	0.64 ± 0.11
rno-miR-539	0.67 ± 0.13
rno-miR-382	0.85 ± 0.12
rno-miR-134	1.64 ± 0.33[***]
rno-miR-485	0.84 ± 0.13
rno-miR-154	0.82 ± 0.12
rno-miR-541	1.49 ± 0.21[***]
miR-17-92 cluster	
rno-miR-17	1.88 ± 0.48
rno-miR-18a	0.50 ± 0.50
rno-miR-20a	1.89 ± 0.23
rno-miR-19b	1.26 ± 0.32
rno-miR-92	2.80 ± 0.89[*]
miR-99a/let-7c/miR-125b-2 cluster	
rno-let-7c	1.45 ± 0.09
rno-miR-99a	2.72 ± 0.51[**]
rno-miR-125b	1.35 ± 0.15
miR-106b-25 cluster	
rno-miR-25	2.15 ± 0.33[**]
rno-miR-93	0.85 ± 0.18

One-way ANOVA and Tukey's HSD post-hoc test were used to calculate significant differences between the indicated miRNA(s) and the remainder of the miRNAs within the same cluster: (*) $P < 0.05$; (**) $P < 0.01$; (***) $P < 0.0001$.
[a]Data are the average of six replicates (± SEM).

TABLE 4. List of selected putative target genes for the abundant and/or enriched axonal miRNAs

	miRNA (A/S ratio of intensity)	
Target gene		
Abbreviation	Accession number	GO annotation
rno-miR-204 (A/S ratio of intensity = 6.92 $\pm$ 0.83)		
Laminin receptor 1 (ribosomal protein SA)		
LAMR1[a,b]	NM_017138.1	Laminin receptor activity
		Cell–cell adhesion
Discs, large homolog 5		
DLG5[a]	NM_001107247.1	Cell–cell adherens junction
Dynein, cytoplasmic, light chain 1		
DNCLC1[a]	NM_053319.2	Neurotransmitter metabolic process
		Nitric oxide biosynthetic process
Glyoxylase 1		
GLO1[a]	NM_207594.1	Glutathione metabolic process
Churchill domain containing 1		
CHURC1[a]	NM_001106741.2	Positive regulation of transcription
rno-miR-221 (A/S ratio of intensity = 5.83 $\pm$ 0.49)		
Tropomyosin 3, γ		
TPM3[a]	NM_057208.2	Actin binding
Kinesin 2		
KNS2[a]	NM_001081973.1	Microtubule motor activity
		Axon cargo transport
Glycoprotein M6A		
GPM6[a]	NM_178105.2	Calcium channel activity
Potassium large conductance calcium-activated channel, subfamily m, β		
KCNMB4[a]	NM_023960.2	Calcium-activated potassium channel activity
Churchill domain containing 1		
CHURC1[a]	NM_001106741.2	Positive regulation of transcription
ADP rybosilation factor 4		
ARF4[b]	NM_024151.1	Epidermal growth factor receptor signaling pathway
		Small GTPase mediated signal transduction
		Vesicle-mediated transport
rno-miR-146 (A/S ratio of intensity = 4.89 $\pm$ 0.35)		
Ribosomal protein L30		
RPL30[a,b]	NM_022699.2	Translation
		Structural constituent of ribosome
Dynein, cytoplasmic, light chain 2A		
DNCL2A[a]	NM_131910.3	Motor activity
		Retrograde axon transport
Aldo-keto reductase family 1, member A1		
AKR1A1[a,b]	NM_031000.3	Alcohol dehydrogenase (NADP+) activity
ATP synthase, H+ transporting, mitochondrial F0 complex, subunit F6		
ATP5J[a]	NM_053602.1	Mitochondrial proton-transporting ATP synthase complex, coupling factor F(o)
CUG triplet repeat, RNA binding protein 2		
CUGBP2[a]	NM_017197.2	mRNA processing
		RNA binding
Syntaxin 7		
STX7[a]	NM_021869.2	Synaptic vesicle exocytosis
		SNAP receptor activity
Casein kinase II, α 1 polypeptide		
CSNK2A1[a]	NM_053824.2	Wnt receptor signaling pathway
		Protein phosphatase activity
Colony stimulating factor 1 receptor		
CSF1R[b]	NM_001029901.1	Transmembrane receptor protein tyrosine kinase signaling pathway
		Protein tyrosine kinase activity

(*continued*)

TABLE 4. *Continued*

miRNA (A/S ratio of intensity)		
Target gene		
Abbreviation	Accession number	GO annotation
Barrier to autointegration factor 1		
BANF1[b]	NM_053631.2	DNA binding
rno-miR-16/15b (A/S ratio of intensity = 3.69 ± 0.35/2.90 ± 0.39)		
Ribosomal protein L32		
RPL32[a]	NM_013226.2	Translation
		Structural constituent of ribosome
Tumor protein, translationally controlled 1		
TPT1[a]	NM_053867.1	Calcium ion binding
Ribosomal protein L41		
RPL41[a,b]	NM_139083.1	Translation
		Structural constituent of ribosome
Kinesin familiy member 5A		
KIF5A[a]	NM_212523.1	Microtubule motor activity
Heterogenous nuclear ribonucleoprotein A1		
HNRPA1[a,b]	NM_017248.1	mRNA transport
		mRNA processing
Mitogen activated protein kinase 8 interacting protein		
MAPK8IP[a]	NM_053777.1	Regulation of JNK cascade
		Kinesin binding
Glutamate receptor, ionotropic, N-methyl D-aspartate- Like 1A		
GRINL1A[a]	NM_183402.1	Transcription
		DNA-directed RNA polymerase activity
rno-miR-320 (A/S ratio of intensity = 2.29 ± 0.24)		
Ribosomal protein L15		
RPL15[a]	NM_139114.3	Translation
		Structural constituent of ribosome
Catenin (cadherin associated protein), β 1, 88 kDa		
CTNNB1[a,b]	NM_053357.2	Regulation of transcription
		Wnt receptor signaling pathway
Zinc finger protein 161		
ZFP161[a]	NM_172325.1	Zinc ion binding
		Protein binding
		Nucleic acid binding
Churchill domain containing 1		
CHURC1[a]	NM_001106741.2	Positive regulation of transcription
Glutamate receptor, ionotropic, N-methyl D-aspartate- Like 1A		
GRINL1A[a]	NM_183402.1	Transcription
		DNA-directed RNA polymerase activity
CDK5 activator binding protein		
CDK5RAP2[b]	XM_575844.2	Neuronal Cdc2-like kinase binding
Tubulin, α 1A		
TUBA1A[b]	NM_022298.1	Microtubule-based movement
		GTPase activity
Peroxiredoxin 1		
PRDX1[b]	NM_057114.1	Cell redox homeostasis
		Response to oxidatve stress
Enolase 1, α		
ENO1[b]	NM_012554.2	Glycolysis
		Phosphopyruvate hydratase activity
Ubiquitin carboxy-terminal hydroxylase L1		
UCHL1[b]	NM_017237.2	Ubiquitin-dependent protein catabolic process
		Ubiquitin thiolesterase activity

(*continued*)

TABLE 4. *Continued*

miRNA (A/S ratio of intensity)		
Target gene		
Abbreviation	Accession number	GO annotation
rno-miR-103 (A/S ratio of intensity = 1.81 ± 0.15)		
Ribosomal protein L32		
RPL32[a]	NM_013226.2	Translation
		Structural constituent of ribosome
Tropomyosin 3, γ		
TPM3[a]	NM_057208.2	Actin binding
Kinesin family member 5A		
KIF5A[a]	NM_212523.1	Microtubule motor activity
		Kinesin complex
Mitogen activated protein kinase 8 interacting protein		
MAPK8IP[a]	NM_053777.1	Regulation of JNK cascade
		Kinesin binding
Kinesin 2		
KNS2[a]	NM_001081973.1	Microtubule motor activity
		Axon cargo transport
Adenylate kinase 2		
AK2[a]	NM_030986.1	Adenine metabolic process
		Adenylate kinase activity
Glutathione peroxidase		
GPX4[a]	NM_017165.2	Phospholipid-hydroperoxide glutathione peroxidase activity
		Mitochondrial inner membrane
Syntaxin 7		
STX7[a]	NM_021869.2	Synaptic vesicle exocytosis
		SNAP receptor activity
Golgi associated, γ adaptin ear containing, ARF binding protein 3		
GGA3[a]	NM_001108304.1	Intracellular protein transport
Cyclin G associated kinase		
GAK[a]	NM_031030.1	Protein amino acid phosphorylation
		Protein serine/threonine kinase activity
Phospolipase C, β 1		
PLCB1[a]	NM_001077641.1	Lipid catabolic process
		Phosphoinositide phospholipase C activity
		Phosphoric diester hydrolase activity
Cysteine-rich protein 2		
CRIP2[a]	NM_022501.1	Zinc ion binding
		Metal ion binding
RAN, member RAS oncogene family		
RAN[a]	NM_053439.1	Microtubule cytoskeleton organization
		GTPase activity
Zinc finger protein 161		
ZFP161[a,b]	NM_172325.1	Zinc ion binding
		Protein binding
		Nucleic acid binding
Churchill domain containing 1		
CHURC1[a]	NM_001106741.2	Positive regulation of transcription
Sterol regulatory element binding factor 2 (predicted)		
SREBF2[a]	NM_001033694.1	Positive regulation of transcription from RNA polymerase II promoter
		Steriod metabolic process
		Response to hormone stimulus
Nuclear factor I/B		
NFIB[a]	NM_031566.1	Regulation of transcription, DNA dependent
Tubulin α A1		
TUBA1A[b]	NM_022298.1	Microtubule-based movement
		GTPase activity

(continued)

TABLE 4. *Continued*

miRNA (A/S ratio of intensity)		
Target gene		
Abbreviation	Accession number	GO annotation
Cystatin 3		
CST3[b]	NM_012837.1	Response to axon injury
		Positive regulation of DNA replication
		Cysteine-type endopeptidase inhibitor activity
Ribosomal protein L41		
RPL41[b]	NM_139083.1	Translation
		Structural constituent of ribosome
Calcium channel, voltage-dependent, L type, α 1C subunit		
CACNA1C[b]	NM_012517.2	Calcium ion transport
		Voltage-gated calcium channel activity
Calpain, small subunit 1		
CAPNS1[b]	NM_017118.1	Calcium ion binding
		Calcium-dependent cysteine-type endopeptidase activity
Thymus cell surface antigen		
THY1[b]	NM_012673.1	Negative regulation of axonogenesis
		Positive regulation of peptidyl-tyrosine phosphorylation
rno-miR-541 (A/S ratio of intensity = 1.49 ± 0.21)		
Arginase type II		
ARG2[a]	NM_019168.1	Arginine metabolic process
rno-miR-125b (A/S ratio of intensity = 1.35 ± 0.15)		
Golgi SNAP receptor member 1		
GOSR1[a]	NM_053584.2	Retrograde transport, endosome to golgi
		ER to golgi vesicle mediated transport
		SNAP receptor activity
Ubiquitin A-52 residue ribosomal protein fusion product 1		
UBA52[a,b]	NM_031687.3	Positive regulation of transcription
Stathmin-like 3		
STMN3[a]	NM_024346.1	Tubulin binding
		Microtubule depolymerization
NADH dehydrogenase (ubiquinone) flavoprotein 3-like		
NDUFV3L[a]	NM_001101011.2	Electron transport chain
		Mitochondrial inner membrane
Dynein, cytoplasmic, light intermediate chain 1		
DNCLI1[a]	NM_145772.1	ATP binding
		Motor activity
Zinc finger protein 161		
ZFP161[a,b]	NM_172325.1	Zinc ion binding
		Protein binding
		Nucleic acid binding
Churchill domain containing 1		
CHURC1[a]	NM_001106741.2	Positive regulation of transcription
Casein kinase II, α 1 polypeptide		
CSNK2A1[a]	NM_053824.2	Wnt receptor signaling pathway
		Protein phosphatase activity
rno-miR-23a,b (A/S ratio of intensity = 1.33 ± 0.12/1.16 ± 0.12)		
Ribosomal protein S23		
RPS23[a,b]	NM_078617.2	Translation
		Structural constituent of ribosome
Up-regulated during skeletal muscle growth 5		
USMG5[a]	NM_133544.1	Integral to membrane
		Mitochondrion

(*continued*)

TABLE 4. *Continued*

miRNA (A/S ratio of intensity)		
Target gene		
Abbreviation	Accession number	GO annotation
Tropomyosin 3, γ		
TPM3[a]	NM_057208.2	Actin binding
Neural precursor cell expressed, developmentally down-regulated gene 8		
NEDD8[a]	NM_138878.2	Regulation of transcription from RNA polymerase II promoter
Myristoylated alanine rich protein kinase C substrate		
MARCKS[a]	M59859.1	Calmodulin binding
		Actin binding
		Protein kinase C binding
CUG triplet repeat, RNA binding protein 2		
CUGBP2[a]	NM_017197.2	mRNA processing
		RNA binding
MARCKS-like protein		
MLP[a]	NM_057144.1	Cellular calcium ion homeostasis
COMM domain containing 3		
COMMD3[a]	NM_198732.1	Protein binding
Basonuclin 2		
BNC2[a]	NM_001106666.1	DNA binding
		Zinc-ion binding
Solute carrier family 25 (mitochondrial carrier; adenine nucleotide translocator), member 4		
SLC25A4[a]	NM_053515.1	Glutamate uptake
		Transmembrane transport
		Adenine nucleotide transmembrane transport activity
CREB binding protein		
CREBBP[a]	NM_133381.2	Positive regulation of transcription from RNA polymerase II promoter
Protein phosphatase 3, catalytic subunit, α isoform		
PPP3CA[a]	NM_017041.1	Regulation of synaptic transmission
		Calcium ion transport
		Phosphoprotein phosphatase activity
Zinc finger protein 161		
ZFP161[a,b]	NM_172325.1	Zinc ion binding
		Protein binding
		Nucleic acid binding
Katanin p60 subunit A-like 1		
KATNAL1[a]	NM_001006956.1	Microtubule-severing
		ATPase activity
		ATP binding
Churchill domain containing 1		
CHURC1[a]	NM_001106741.2	Positive regulation of transcription
Casein kinase II, α 1 polypeptide		
CSNK2A1[a]	NM_053824.2	Wnt receptor signaling pathway
		Protein phosphatase activity
Glutamate receptor, ionotropic, N-methyl D-aspartate- Like 1A		
GRINL1A[a]	NM_183402.1	Transcription
		DNA-directed RNA polymerase activity
Neurofilament, light polypeptide		
NEFL[b]	NM_031783.1	Anterograde axon cargo transport
		Retrograde axon cargo transport
		Axon transport of mitochondria
Myosin regulatory light chain (RLC-B)		
MRLC2[b]	NM_017343.2	Motor activity
		Calcium ion binding

(continued)

TABLE 4. *Continued*

miRNA (A/S ratio of intensity)		
Target gene		
Abbreviation	Accession number	GO annotation
rno-miR-26a (A/S ratio of intensity = 1.24 ± 0.06)		
Catenin (cadherin associated protein), β 1, 88 kDa		
CTNNB1[a,b]	NM_053357.2	Regulation of transcription Wnt receptor signaling pathway
Cytochrome c oxidase subunit VA		
COX5A[a]	NM_145783.1	Cytochrome c oxidase activity
Tyrosine 3-monooxygenase/tryptophan 5-monooxygenase activation protein, ε polypeptide		
YWHAE [a]	NM_031603.1	Protein kinase C inhibitor activity
Microtubule associated protein 1B		
MAP1b[a,b]	NM_019217.1	Negative regulation of microtubule depolymerization Microtubule binding
Transmembrane emp24-like trafficking protein 10		
TMED10[b]	NM_053467.1	Intracellular protein transport Vesicle mediated transport
rno-miR-382 (A/S ratio of intensity = 0.85 ± 0.12)		
Ribosomal protein L32		
RPL32[a]	NM_013226.2	Translation Structural constituent of ribosome
Ribosomal protein S11		
RPS11[a,b]	NM_031110.1	Translation Structural constituent of ribosome
ATP synthase, H+ transporting, mitochondrial F1 complex, γ polypeptide 1		
ATP5C1[a,b]	NM_053825.1	Oxidative phosphorylation ATP biosynthetic process Proton-transporting ATPase activity, rotational mechanism
Nerve growth factor receptor (TNFRS16) associated protein 1		
NGFRAP1[a]	NM_053401.1	Induction of apoptosis via death domain receptors
Ribosomal protein S11		
RPS11[b]	NM_031110.1	Translation Structural constituent of ribosome
Ribosomal protein L15		
RPL15[a,b]	NM_139114.3	Translation Structural constituent of ribosome
rno-miR-24 (A/S ratio of intensity = 0.84 ± 0.11)		
Dynein, cytoplasmic, light intermediate chain 1		
DNCLI1[a]	NM_145772.1	ATP binding Motor activity
Pyroglutamyl-peptidase 1		
PGPEP1[a]	NM_201988.2	Proteolysis Cysteine-type peptidase activity
Parkinson disease 7		
PARK7[a]	NM_057143.1	Response to oxidative stress
Translocase of inner mitochondrial membrane 13 homolog		
TIMM13[a]	NM_145781.1	Protein import into mitochondrial inner membrane Transmembrane transport
Matrin 3		
MATR3[a]	NM_019149.2	RNA binding Zinc ion binding
Churchill domain containing 1		
CHURC1[a]	NM_001106741.2	Positive regulation of transcription

(continued)

TABLE 4. *Continued*

miRNA (A/S ratio of intensity)		
Target gene		
Abbreviation	Accession number	GO annotation
Glutamate receptor, ionotropic, N-methyl D-aspartate- Like 1A		
GRINL1A[a]	NM_183402.1	Transcription
		DNA-directed RNA polymerase activity
Sterol regulatory element binding factor 2 (predicted)		
SREBF2[a]	NM_001033694.1	Specific RNA polymerase II transcription factor activity
		Steriod metabolic process
		Response to hormone stimulus
Neurofilament, medium polypeptide		
NEFM[b]	NM_017029.1	Neurofilament cytoskeleton organization
		Axon cargo transport
	rno-miR-185 (A/S ratio of intensity = 0.62 ± 0.05)	
Dynein, cytoplasmic, light chain 2A		
DNCL2A[a]	NM_131910.3	Motor activity
		Retrograde axon transport
ATPase, H+ transporting, V1 subunit F		
ATP6V1F[a]	NM_053884.1	Proton transport
		ATP synthesis coupled protein transport
		ATPase activity, coupled to transmembrane movement of ions
COP9 constitutive photomorphogenic homolog subunit 4		
COPS4[a]	NM_001004275.1	Protein binding
Cyclin G associated kinase		
GAK[a]	NM_031030.1	Protein amino acid phosphorylation
		Protein serine/threonine kinase activity
Trans-2,3-enoyl-CoA reductase		
GPSN2[a]	NM_138549.1	Lipid biosynthetic process
		Oxidoreductase activity
Cysteine-rich protein 2		
CRIP2[a]	NM_022501.1	Zinc ion binding
		Metal ion binding
Glutamate receptor, ionotropic, N-methyl D-aspartate- Like 1A		
GRINL1A[a]	NM_183402.1	Transcription
		DNA-directed RNA polymerase activity
CD63 antigen		
CD63[b]	NM_017125.3	Positive regulation of cell adhesion
		Positive regulation of endocytosis
Cytochrome b-245, β polypeptide		
CYBB[b]	NM_023965.1	Oxidation reduction
		NAD(P)H oxidase activity
Barrier to autointegration factor 1		
BANF1[b]	NM_053631.2	DNA binding

Note: A/S indicates axon/soma.
[a]Presence of the mRNA in the axon previously reported by Taylor et al (2009).
[b]Presence of the mRNA in the axon previously reported by Willis et al (2007).

Campenot compartmented culture dishes as previously described (Hillefors et al. 2007). Cells were cultured in serum-free medium containing 20 mM KCl, NGF (50 ng/mL), and 20 U/mL Penicillin/20 μg/mL Streptomycin (Hyclone) for 3–10 d prior to use, with media changes every 3–4 d. To inhibit the proliferation of nonneuronal cells, 5-fluoro-2′-deoxyuridine (50 nM) was added to the culture medium 24 h after plating and maintained throughout the culture period. The side compartments, which contained the distal axons used in these experiments, contained no neuronal soma or non-neuronal cells, as judged by phase-contrast microscopy, as well as ethidium bromide and acridine orange staining.

Western blot analysis

Distal axons in the side compartments of Campenot chambers or soma and proximal axons in the central compartment were harvested separately and lysed in 50 mM Tris-HCl (pH 7.4),

150 mM NaCl, 1 mM EDTA, 1% NP-40, and Complete protease inhibitor cocktail (Roche). Protein concentration was assessed using the Micro BCA Protein Assay Kit (Pierce). For SDS-PAGE, equal amounts (2–5 μg) of each lysate were boiled in NuPage sample buffer (Invitrogen) and resolved on 4%–12% linear gradient gels. Proteins were transferred to PVDF membranes, probed with monoclonal antibodies to β-actin, Tau, and MAP2 (Sigma), and developed using the ECL Advance Western Blotting Detection Kit (GE Health Care).

In situ hybridization

Visualization of miR-16 and miR-221 in the axons of SCG neurons was accomplished by in situ hybridization using fluorescein isothiocyanate (FITC)-conjugated LNA probes (25 nM, Exiqon). A scrambled miR probe was employed as a negative control. We followed the protocol described in Aschrafi et al. (2010), with the following modifications. After fixation, the neurons were dehydrated and rehydrated by sequential addition of 70%, 90%, 100%, 90%, and 70% ethanol solutions, and washed three times in PBS. After hybridization, the neurons were washed twice in 2×SSC and twice in 0.2×SSC at 60°C, for 30 min each. The signal intensity of the FITC probe was amplified with the Alexa Fluor 488 Signal Amplification Kit (Molecular Probes).

RNA isolation and miRNA microarray analyses

Total RNA was isolated from the axons or soma of SCG neurons using RiboZol RNA extraction reagent (Amresco) according to the manufacturer's protocol. The concentration and purity of the RNA were assessed using a UV spectrophotometer. Total RNA samples, isolated from the central and side compartments of the Campenot chambers, were analyzed using the NCode Multi-Species miRNA microarray kit (Invitrogen). MicroRNA populations were polyadenylated and subsequently ligated to labeled DNA polymers using the 6X Alexa Fluor 3 (A3) or 6X Alexa Fluor 5 (A5) Rapid Ligation Mix. The two differentially labeled reactions were combined into one tube and then loaded onto NCode Multi-Species miRNA Microarray V2. The arrays were mounted with the Maui Mixer SL and hybridized overnight (16–20 h) at 52°C with constant mixing. The arrays were washed and scanned using a GenePix 4000B microarray scanner (Molecular Devices). The scanned array images were then annotated and analyzed using the GenePix software. The annotated data were normalized using a Latin Squares algorithm by the NCode Profiler data analysis software. A dye swap analysis was performed on the data to identify differential markers. The array data were checked to ensure the median backgrounds were below 75 relative fluorescent units (RFU). Median local backgrounds were subtracted from the median spot intensities to generate background-corrected median intensities for all spots.

Quantitative RT-PCR

For optimized detection and quantification of miRNAs, cDNA was synthesized from total RNA using the NCode miRNA First Strand cDNA synthesis kit (Invitrogen) according to the manufacturer's protocol. Using first-strand cDNA as a template, triplicate qPCR reactions were performed for each miRNA using miRNA-specific forward primers and the NCode Universal qPCR reverse primer. The forward primers for qPCR analyses for each

miRNA were designed using the entire mature miRNA sequence. Minus template and minus forward primer controls were included to ensure lack of signal in the assay background. All C_T values used for analyses were averaged from three to six replicates and those with high standard deviation (>1) were not included in the analyses. Melting curve analysis was performed to test for the specificity and quality of the qPCR amplifications. Relative expression was calculated using the comparative C_T method and normalized to the expression of U6 snRNA and miR-103. Using miR-221 as an example, the relative expression (RQ) was calculated as follows:

$$\Delta\Delta C_T = \Delta C_{T,axon} - \Delta C_{T,soma} = \left[C_{T,miR\text{-}221} - C_{T,U6}\right]_{axon}$$
$$- \left[C_{T,miR\text{-}221} - C_{T,U6}\right]_{soma} = [31.41 - 29.45]$$
$$- [25.39 - 23.97] = 1.92 - 2.41 = -0.49,$$

where relative expression (or RQ) $= 2^{-\Delta\Delta C_T} = 2^{-(-0.49)} = 1.41$.

RT-PCR methodology was also used to assess the purity of the axonal RNA preparations. In these experiments, total RNA was reverse transcribed using oligo (dT) primers and SuperScript First-Strand Synthesis Kit (Invitrogen). Amplification was accomplished using gene-specific primers as previously described (Gioio et al. 2001). PCR reactions for synaptic vesicle associated proteins and GFAP were fractionated by electrophoresis on 2.5% agarose gels, and amplicons were visualized by ethidium bromide staining. PCR reactions without reverse transcriptase yielded no amplification products.

Statistical analysis

Student's *t*-test was used to determine significant differences between two groups. One-way ANOVA and Tukey's HSD post-hoc test were used to analyze significant differences among multiple groups; $P < 0.05$ was considered significant.

SUPPLEMENTAL MATERIAL

Supplemental material can be found at http://www.rnajournal.org.

ACKNOWLEDGMENTS

REFERENCES

Aldrich BT, Frakes EP, Kasuya J, Hammonda DL, Kitamoto T. 2009. Changes in expression of sensory organ-specific microRNAs in rat dorsal root ganglia in association with mechanical hypersensitivity induced by spinal nerve ligation. *Neuroscience* **164:** 711–723.

Ambros V, Lee RC. 2004. Identification of microRNAs and other tiny noncoding RNAs by cDNA cloning. *Methods Mol Biol* **265:** 131–158.

Aschrafi A, Schwechter AD, Mameza MG, Natera-Naranjo O, Gioio AE, Kaplan BB. 2008. MicroRNA-338 regulates local cytochrome

c oxidase IV mRNA levels and oxidative phosphorylation in the axons of sympathetic neurons. *J Neurosci* **28:** 12581–12590.

Aschrafi A, Natera-Naranjo O, Gioio AE, Kaplan BB. 2010. Regulation of axonal trafficking of cytochrome *c* oxidase IV mRNA. *Mol Cell Neurosci* **43:** 422–430.

Bassell GJ, Warren ST. 2008. Fragile X syndrome: Loss of local mRNA regulation alters synaptic development and function. *Neuron* **60:** 201–214.

Bi J, Tsai NP, Lin YP, Loh HH, Wei LN. 2006. Axonal mRNA transport and localized translational regulation of κ-opioid receptor in primary neurons of dorsal root ganglia. *Proc Natl Acad Sci* **103:** 19919–19924.

Costa-Mattioli M, Sossin WS, Klann E, Sonenberg N. 2009. Translational control of long-lasting synaptic plasticity and memory. *Neuron* **61:** 10–26.

Crispino M, Cefaliello C, Kaplan B, Giuditta A. 2009. Protein synthesis in nerve terminals and the glia-neuron unit. In *Cell biology of the axon* (ed. E Koenig), pp.246–267. Springer, Berlin, Germany.

Filipowicz W, Bhattacharyya SN, Sonenberg N. 2008. Mechanisms of post-transcriptional regulation by microRNAs: Are the answers in sight? *Nat Rev Genet* **9:** 102–114.

Gioio AE, Eyman M, Zhang H, Lavina ZS, Giuditta A, Kaplan BB. 2001. Local synthesis of nuclear-encoded mitochondrial proteins in the presynaptic nerve terminal. *J Neurosci Res* **64:** 447–453.

Hébert SS, Horré K, Nicolaï L, Bergmans B, Papadopoulou AS, Delacourte A, De Strooper B. 2009. MicroRNA regulation of Alzheimer's amyloid precursor protein expression. *Neurobiol Dis* **33:** 422–428.

Hillefors M, Gioio AE, Mameza MG, Kaplan BB. 2007. Axon viability and mitochondrial function are dependent on local protein synthesis in sympathetic neurons. *Cell Mol Neurobiol* **27:** 701–716.

Huang F, Chotiner JK, Steward O. 2005. The mRNA for elongation factor 1α is localized in dendrites and translated in response to treatments that induce long-term depression. *J Neurosci* **25:** 7199–7209.

Hunsberger JG, Austin DR, Chen G, Manji HK. 2009. MicroRNAs in mental health: From biological underpinnings to potential therapies. *Neuromolecular Med* **11:** 173–182.

Kaplan BB, Gioio AE, Hillefors M, Aschrafi A. 2009. Axonal protein synthesis and the regulation of local mitochondrial function. In *Cell biology of the axon* (ed. E Koenig), pp.225–242. Springer, Berlin, Germany.

Kim VN. 2005. MicroRNA biogenesis: Coordinated cropping and dicing. *Nat Rev Mol Cell Biol* **6:** 376–385.

Klann E, Antion MD, Banko JL, Hou L. 2004. Synaptic plasticity and translation initiation. *Learn Mem* **11:** 365–372.

Kosik KS. 2006. The neuronal microRNA system. *Nat Rev Neurosci* **7:** 911–920.

Kye MJ, Liu T, Levy SF, Xu NL, Groves BB, Bonneau R, Lao K, Kosik KS. 2007. Somatodendritic microRNAs identified by laser capture and multiplex RT-PCR. *RNA* **13:** 1224–1234.

Lagos-Quintana M, Rauhut R, Meyer J, Borkhardt A, Tuschl T. 2003. New microRNAs from mouse and human. *RNA* **9:** 175–179.

Lewis BP, Burge CB, Bartel DP. 2005. Conserved seed pairing, often flanked by adenosines, indicates that thousands of human genes are microRNA targets. *Cell* **120:** 15–20.

Li Y, Park JS, Deng JH, Bai Y. 2006. Cytochrome c oxidase subunit IV is essential for assembly and respiratory function of the enzyme complex. *J Bioenerg Biomembr* **38:** 283–291.

Lugli G, Torvik VI, Larson J, Smalheiser NR. 2008. Expression of microRNAs and their precursors in synaptic fractions of adult mouse forebrain. *J Neurochem* **106:** 650–661.

Martin KC. 2004. Local protein synthesis during axon guidance and synaptic plasticity. *Curr Opin Neurobiol* **14:** 305–310.

Merianda TT, Lin AC, Lam JS, Vuppalanchi D, Willis DE, Karin N, Holt CE, Twiss JL. 2009. A functional equivalent of endoplasmic reticulum and Golgi in axons for secretion of locally synthesized proteins. *Mol Cell Neurosci* **40:** 128–142.

Niwa R, Slack FJ. 2007. The evolution of animal microRNA function. *Curr Opin Genet Dev* **17:** 145–150.

Obernosterer G, Leuschner PJ, Alenius M, Martinez J. 2006. Post-transcriptional regulation of microRNA expression. *RNA* **12:** 1161–1167.

Peltier HJ, Latham GJ. 2008. Normalization of microRNA expression levels in quantitative RT-PCR assays: Identification of suitable reference RNA targets in normal and cancerous human solid tissues. *RNA* **14:** 844–852.

Saba R, Goodman CD, Huzarewich RL, Robertson C, Booth SA. 2008. A miRNA signature of prion induced neurodegeneration. *PLoS ONE* **3:** e3652. doi: 10.1371/journal.pone.0003652.

Schmittgen TD, Livak KJ. 2008. Analyzing real-time PCR data by the comparative C_T method. *Nat Protoc* **3:** 1101–1108.

Schmittgen TD, Lee EJ, Jiang J, Sarkar A, Yang L, Elton TS, Chen C. 2008. Real-time PCR quantification of precursor and mature microRNA. *Methods* **44:** 31–38.

Schratt G. 2009a. Fine-tuning neural gene expression with micro-RNAs. *Curr Opin Neurobiol* **19:** 213–219.

Schratt G. 2009b. MicroRNAs at the synapse. *Nat Rev Neurosci* **10:** 842–849.

Siegel G, Obernosterer G, Fiore R, Oehmen M, Bicker S, Christensen M, Khudayberdiev S, Leuschner PF, Busch CJ, Kane C, et al. 2009. A functional screen implicates microRNA-138-dependent regulation of the depalmitoylation enzyme APT1 in dendritic spine morphogenesis. *Nat Cell Biol* **11:** 705–716.

Smart F, Aschrafi A, Atkins A, Owens GC, Pilotte J, Cunningham BA, Vanderklish PW. 2007. Two isoforms of the cold-inducible mRNA-binding protein RBM3 localize to dendrites and promote translation. *J Neurochem* **101:** 1367–1379.

Spencer GE, Syed NI, van Kesteren E, Lukowiak K, Geraerts WP, van Minnen J. 2000. Synthesis and functional integration of a neurotransmitter receptor in isolated invertebrate axons. *J Neurobiol* **44:** 72–81.

Taylor AM, Berchtold NC, Perreau VM, Tu CH, Li JN, Cotman CW. 2009. Axonal mRNA in uninjured and regenerating cortical mammalian axons. *J Neurosci* **29:** 4697–4707.

Tsai NP, Bi J, Loh HH, Wei LN. 2006. Netrin-1 signaling regulates de novo protein synthesis of κ opioid receptor by facilitating polysomal partition of its mRNA. *J Neurosci* **26:** 9743–9749.

van Rooij E, Olson EN. 2007. microRNAs put their signatures on the heart. *Physiol Genomics* **31:** 365–366.

Vogelaar CF, Gervasi NM, Gumy LF, Story DJ, Raha-Chowdhury R, Leung KM, Holt CE, Fawcett JW. 2009. Axonal mRNAs: Characterization and role in the growth and regeneration of dorsal root ganglion axons and growth cones. *Mol Cell Neurosci* **42:** 102–115.

Willis DE, van Niekerk EA, Sasaki Y, Mesngon M, Merianda TT, Williams GG, Kendall M, Smith DS, Bassell GJ, Twiss JL. 2007. Extracellular stimuli specifically regulate localized levels of individual neuronal mRNAs. *J Cell Biol* **178:** 965–980.